Palestine Journal of Mathematics

Vol.15(3), (2026) , 423–433 © Palestine Polytechnic University-PPU 2026

Solution of Fractional Mathieu Differential Equations using Haar Wavelet

A. M. Jarrah, Jay Kishore Sahani and Pankaj Sharma

Communicated by Geeta Arora

MSC 2020 Classifications: 65N99; 65T60; 26A33.

Keywords and phrases: Wavelets, Fractional calculus, Fractional Mathieu equations, Operational matrix.

The authors would like to thank the reviewers and editor for their constructive comments and valuable suggestions that improved the quality of our paper.

Corresponding Author: Pankaj Sharma

Abstract. In this paper, we introduce a computationally efficient method utilizing the Haar wavelet technique to solve fractional Mathieu differential equations. By employing fractional operational matrix of integration and truncated Haar wavelet expansions, we transform these equations into a system of algebraic equations, which are then simplified to find the unknown coefficients. From tables and figures in the present work, we see that the proposed approach is computationally efficient. It may be more suitable for solving a diverse range of nonlinear fractional differential equations encountered in science and engineering. Numerical examples illustrate the better accuracy of our proposed method across diverse conditions.

1 Introduction

Differential equations play a fundamental role in modern science and engineering, serving as the basis for many known laws of physics, chemistry, and other natural sciences [2, 3]. They are extensively employed in various fields, including biology, where they are used to model biochemical reactions, population dynamics, organism growth, and the spread of diseases. A mathematical model serves as a description of real-world systems using mathematical concepts and language. Mathematical models represented by differential equations play a fundamental role in describing a wide range of physical phenomena across various scientific disciplines, including electromagnetism, elastic wave equations, frequency modulation, parametric oscillators, mirror traps for neutral particles, and the motion of quantum particles in periodic potentials [12]. Differential equations are known to accurately describe numerous physical phenomena, including electromagnetic interactions, wave equations with elliptical boundary conditions (as seen in waveguides or resonators), particle motion in alternating gradient focusing or electromagnetic traps, parametric oscillators, motion of quantum particles in periodic potentials, and eigenfunctions of the quantum pendulum [12]. Among these equations, the homogeneous second-order Mathieu differential equation is particularly notable for its widespread use in modeling such phenomena. The Mathieu differential equation, as introduced by the renowned French mathematician Mile Lonard Mathieu [4], represents a significant nonlinear differential equation governing phenomena such as the vibration modes of elliptic membranes. The equation is defined as follows:

$$y''(x) + (a - 2qcos(x))y(x) = 0. \tag{1.1}$$

where, a and q denote the characteristic number and parameter, respectively. When the characteristic parameter $q = 0$, equation (1.1) simplifies to a simple harmonic oscillator, exhibiting free vibration around the stable equilibrium position $y = 0$. For non-zero characteristic parameters, equation (1.1) may or may not possess stable solutions [1]. The stability or instability of equation (1.1) can be determined by selecting appropriate values for q and a.

Rand et al. [5] investigated the regions of stability and instability, delineated by transition curves. Younesian et al. [6] provided an asymptotic solution and delineated transition curves for the non-homogeneous Mathieu equation. A stability chart for equation (1.1) was constructed using an efficient numerical scheme in [7]. Kalas et al. [8] proposed the existence of periodic and quasiperiodic solutions for the generalized Van der Pol-Mathieu equation using the averaging method. Kovacic et al. [9] outlined a method to determine the corresponding stability chart for equation (1.1). Wilkinson et al. [10] and other researchers [12, 11] provided various approximations, along with their accuracy and applicable regions. Recently, Ruihong Mu et al. [13] investigated the stability of the fractional-order Mathieu Equation under forced excitation.

A modern tool widely utilized for describing various physical and mathematical phenomena is fractional calculus. Unlike integer-order models, fractional derivatives provide insights into the memory and hereditary properties of materials modeled in a fractional manner [14].

The general fractional form of Mathieu equation (1.1), given in [5], is written as:

$$D^{\beta}y(x) + kD^{\alpha}y(x) + (a - 2qcos(x))y(x) = f(x), \quad 0 \leq \alpha \leq 1 \quad 0 \leq \beta \leq 2. \tag{1.2}$$

In equation (1.2), D^{β} and D^{α} denote Caputo derivative operators, k is a constant known as damping force, a is characteristic number and q is characteristic parameter of the equation. When $\alpha = 1$ and $\beta = 2$, equation (1.2) transforms into the Mathieu Damped equation, as mentioned in [15]. Details on Caputo derivatives can be found in Rand et al. [5]. Various authors have numerically solved the fractional Mathieu equation using different methods. Rand et al. [5] applied the harmonic balance method, while Abdelhalim et al. [16] utilized the Adomian decomposition and series method for equation (1.2) with a damped term. Najafi et al. [15] proposed the generalized differential transform method, and Wen et al. [17] elucidated the dynamics of the Mathieu equation with two types of fractional-order Van der Pol (VDP) terms. The Block-Pulse wavelets approximation method was introduced in [12], and Hojjat et al. [11] employed radial basis functions for the numerical solution of the fractional Mathieu equation.

This research paper presents a computational approach based on the Haar wavelet collocation method for solving a general form of the fractional Mathieu differential equation (1.2). We have transformed the domain of fractional Mathieu equation from $[0, 80]$ to $[0, 1]$ to visualize the change in behavior of solution of equation. The methodology employs the Haar wavelet for numerical approximation compare to those in [18]. The paper is structured into four sections: Section 2 provides preliminary concepts and terminology, along with Haar family functions, its matrix formulation, and the corresponding operational matrix. Section 3 details the methodology, while Section 4 presents convergence analysis, followed by results and a concluding discussion on the findings. Finally, conclusion is in the last section. This article aims to provide a better simulation of the solution of the general form of the fractional Mathieu equation using the proposed scheme.

2 Preliminary Concepts and Terminology

2.1 Fractional Calculus

Fractional differential equations have gained significant prominence in various scientific disciplines, particularly in physics and mechanics. The Riemann-Liouville fractional derivative [14] of order α with respect to the variable t, starting from $t = a$, is defined as:

$${}_aD_t^{\alpha}f(t) = \begin{cases} \frac{1}{\Gamma(1+m-\alpha)}\frac{d^{m+1}}{dt^{m+1}}\int_a^t (t-x)^{(m-\alpha)}f(x)dx & 0 \leq m \leq \alpha < m+1 \\ \frac{d^{m+1}}{dt^{m+1}}f(t), & \alpha = m+1 \text{ and } \alpha \in \mathbb{N}. \end{cases} \tag{2.1}$$

The definition of the Riemann-Liouville fractional integration of order α, as per [14], is given by:

$$I^{\alpha}f(t) = {}_a\, D_t^{-\alpha}f(t) = \frac{1}{\Gamma(\alpha)}\int_a^t (t-x)^{(\alpha-1)}f(x)dx \qquad \alpha > 0, \tag{2.2}$$

whereas the Caputo fractional derivative [14] of $f \in L^1[0,1]$, is defined as follows:

$$D^{\alpha} f(t) = \begin{cases} I^{n-\alpha} D^{\alpha} f(t) & n-1 \leq \alpha \leq n \quad n \in \mathbb{N} \quad t > 0. \\ \frac{d^n}{dt^n} f(t), & \alpha = n \end{cases} \tag{2.3}$$

The connection between the Caputo operator and Riemann-Liouville [12] is illustrated by the following equations:

$$ {}_a D_t^{\alpha} I^{\alpha} f(t) = f(t), \tag{2.4}$$

$$I_a^{\alpha} D_t^{\alpha} f(t) = f(t) - \sum_{k=0}^{n-1} f(k)(a^+) \frac{(t-\alpha)^k}{k!}, \quad t > 0. \tag{2.5}$$

2.2 Haar wavelets

Wavelets are derived from a foundational function referred to as the “mother wavelet" through dilation and translation processes. In cases where both translational and dilational variables are continuous, the continuous family of wavelets is defined as follows [21, 22]:

$$\psi_{a,b}(x) = |a|^{-\frac{1}{2}} \psi\left(\frac{x-b}{a}\right), \quad a, b \in \mathbb{R}, \quad a \neq 0.$$

Restricting the variables a and b to discrete values, the discrete wavelet family is characterized by $a = a_0^{-m}$ and $b = nb_0 a_0^{-m}$, where $a_0 > 1$ and $b_0 > 1$, with n and m denoting natural numbers. Therefore,

$$\psi_{a,b}(x) = |a_0|^{\frac{m}{2}} \, \psi\left(a_0^m x - nb_0\right),$$

where $\psi_{a,b}(x)$ is a basis (wavelet basis) of $L^2(\mathbb{R})$, represents discrete family of wavelets. In particular, when $a_0 = 2$ and $b_0 = 1$, then $\psi_{a,b}(x)$ forms an orthonormal basis.
Haar function was first time introduced by Alfred Haar in 1910. The first haar wavelet is define as:

$$h_0(x) = \begin{cases} 1, & 0 \leq x < 1 \\ 0, & \text{otherwise.} \end{cases} \tag{2.6}$$

The other Haar wavelets are defined within the interval $[0,1]$, and they are described as follows [20]:

$$h_n(x) = h\left(2^j x - \frac{k}{2^j}\right), \tag{2.7}$$

where, $n = 2^j + k$, $j \geq 0, 0 \leq k \leq 2^j$ and $h(x)$ is define as

$$h(x) = \begin{cases} 1, & 0 \leq x < \frac{1}{2} \\ -1, & \frac{1}{2} \leq x < 1 \\ 0, & \text{otherwise.} \end{cases} \tag{2.8}$$

The expressions for the first and second integral of the Haar family function, as defined in [19], are given by:

$$p_{1,i}(x) = \int_0^x h_i(t)dt = \begin{cases} x-a, & a \leq x < b \\ c-x, & b \leq x < c \\ 0, & \text{otherwise,} \end{cases} \tag{2.9}$$

and

$$p_{2,i}(x) = \int_0^x p_{1,i}(t)dt = \begin{cases} 0, & 0 \leq x < a \\ \frac{(x-a)^2}{2}, & a \leq x < b \\ \frac{1}{4m^2} - \frac{(c-x)^2}{2}, & b \leq x < c \\ \frac{1}{4m^2}, & c \leq x < 1. \end{cases} \tag{2.10}$$

2.3 Function approximation and operational matrix of fractional integration

Any continuous function $f(x) \in L^2(\mathbb{R})$ on the interval $[0, 1)$ can be expressed as

$$f(x) = \sum_{i=0}^{\infty} c_i h_i(x), \tag{2.11}$$

where, $c_i = (2^{j-1}) \int_0^1 u(x)h_i(x)dx$. If the infinite series in equation (2.11) is truncated upto n, then it can be written as

$$f(x) = \sum_{i=0}^{n-1} c_i h_i(x) = C^T h(x), \tag{2.12}$$

where, C and $h(x)$ are given by $C = [c_1, c_2, \dots c_m]^T$ and $h(x) = [h_1(x), h_2(x), \dots h_i(x)]^T$. Now, the fractional integration [12] of the function $f(x)$ is defined as

$$I^{\alpha}(C^T h(x)) = C^T F^{(\alpha)} h(x), \tag{2.13}$$

where, F^{α} is the operational matrix of fractional order integration which is define as

$$F^{\alpha} = (\frac{1}{m})^{\alpha} \frac{1}{\Gamma(\alpha+2)} \begin{pmatrix} 1 & \zeta_1 & \zeta_2 & \dots & \zeta_{m-1} \\ 0 & 1 & \zeta_1 & .. & \zeta_{m-2} \\ 0 & 0 & 1 & .. & \zeta_{m-3} \\ .. & .. & .. & \dots & \dots \\ 0 & 0 & 0 & .. & 1 \end{pmatrix}, \tag{2.14}$$

with $\zeta_k = (k+1)^{\alpha} - 2k^{\alpha+1} + (k-1)^{\alpha+1}, \quad k = 1, 2, ...m-1.$

3 Methodology

Let us consider the Fractional Mathieu equation

$$D^{\beta}y(x) + kD^{\alpha}y(x) + (a - 2qcos(2x))y(x) = f(x),$$

with the initial conditions, $y(0) = \alpha 1$ and $y'(0) = \beta 1$. Let

$$D^{\beta}y(x) = \sum_{i=0}^{n-1} c_i h_i(x) = C^T h(x). \tag{3.1}$$

Now, from equation (3.1) and by [12], we get the following:

$$D^{\alpha}y(x) = I^{(\beta-\alpha)}D^{\beta}y(x) = I^{(\beta-\alpha)}(C^T h(x)) = C^T F^{(\beta-\alpha)}h(x) + \beta 1. \tag{3.2}$$

On integrating the equation (3.2), we get

$$y(x) = C^T F^{\beta} h(x) + \beta 1x + \alpha 1. \tag{3.3}$$

As a result, equation (1.2) transforms into

$$C^T h(x) + k(C^T F^{(\beta-\alpha)}h(x) + \beta 1) + (a - 2qcos(2x))(C^T F^{\beta}h(x) + \beta 1x + \alpha 1) = f(x).$$

Therefore,

$$C^T(h(x) + kF^{(\beta-\alpha)}h(x) + (a - 2qcos(2x))F^{\beta}h(x)) = g(x), \tag{3.4}$$

where, $g(x) = f(x) - k\beta 1 - (a - 2qcos(2x))(\alpha 1 + x\beta 1)$.

Now, collocating $x_j = \frac{j-1}{N}$, $j = 1, 2, 3, ..., N$, we get the system of algebraic equations which is solved for the values of the unknown vector C. Subsequently, by substituting these values of c_i into equation (3.4), we derive the Haar wavelet approximate solution for the given problem.

4 Convergence analysis, results and discussion

This section delve the convergence analysis, results and discussion of the proposed method.

Theorem 4.1. *The approximate solution of the fractional derivative in equation (1.2) through the Haar wavelet converges to its exact solution.*

Proof. Consider $D^{\beta}y(x) = C^{T}h(x)$. Then by equations (2.12) and (3.1), we can write the absolute error e as:

$$e = ||y(x) - (C^{T}F^{\alpha}h(x) + \sum_{k=0}^{m-1} y^{(}k)(a^{+})\frac{(x)^{k}}{k!})||.$$

Also from equation (2.5), we have:

$$e = ||(I^{\beta}(D^{\beta}y(x)) + \sum_{k=0}^{m-1} y^{(}k)(a^{+})\frac{(x)^{k}}{k!}) - (C^{T}F^{\alpha}h(x) + \sum_{k=0}^{m-1} y^{(}k)(a^{+})\frac{(x)^{k}}{k!})||,$$

which gives the absolute error

$$e = ||(I^{\beta}(D^{\beta}y(x)) - (C^{T}F^{\alpha}h(x)|| = I^{\beta}||D^{\beta}y(x) - C^{T}h(x)|| \leq I^{\beta}(C/m).$$

Therefore, e tends to zero as $m \to \infty$. □

We will explore the test problems in three distinct cases:

Case-A : When damping forces $k \neq 0$ and the characteristic parameter $q \neq 0$.

Case-B : This scenario involves damping forces $k = 0$ and a non-zero characteristic parameter q.

Case-C : Here, we consider damping forces $k \neq 0$ along with a characteristic parameter $q = 0$.

4.1 Problem 1 [Case-A]

Consider the problem given by equation (1.2) with the following parameters: $k = 1$, $\alpha = 1$, $\beta = 2$, $f(x) = e^{-x}$, $q = 0$, and $a = 1$. Additionally, we have the initial values $y(0) = \alpha 1 = 1$ and $y'(0) = \beta 1 = -1$. The exact solution to this problem is $y(x) = e^{-x}$. Let

$$D^{\beta}y(x) = C^{T}h(x). \tag{4.1}$$

Then,

$$D^{\alpha}y(x) = C^{T}F^{(\beta-\alpha)}h(x) - 1,$$

and

$$y(x) = C^{T}F^{\beta}h(x) + 1 - x. \tag{4.2}$$

Therefore, problem 1 becomes,

$$C^{T}h(x) + (C^{T}F^{(\beta-\alpha)}h(x) - 1) + (C^{T}F^{\beta}h(x) + 1 - x) = e^{-x},$$

which can be further written as,

$$C^{T}(h(x) + F^{(\beta-\alpha)}h(x) + (a - 2qcos(2x))F^{\beta}h(x)) = e^{-x} + 1 - (1 - x). \tag{4.3}$$

Hence, by implementing the procedure outlined in Section 3, we derive a system of equations which are further solved to obtain the optimal wavelet coefficients. The values obtained by exact solution and proposed method are depicted in figure 1 and error analysis has been depicted in figure 2.

The approximate values acquired through this method are mentioned in Table 1 for comparison.

Table 1. Comparative analysis of approximate values with exact solution.

t	Exact solution	HWS	Absolute error
0/16	0.9692	0.9694	0.1480 e − 3
1/16	0.9105	0.9106	0.1199 e − 03
2/16	0.8553	0.8554	0.0943 e − 03
3/16	0.8035	0.8036	0.0708 e − 03
4/16	0.7548	0.7549	0.0495 e − 03
5/16	0.7091	0.7091	0.0303e − 03
6/16	0.6661	0.6662	0.0130 e − 03
7/16	0.6258	0.6258	0.0025 e − 03
8/16	0.5879	0.5879	0.0163 e − 03
9/16	0.5523	0.5522	0.0285 e − 03
10/16	0.5188	0.5188	0.0391 e − 03
11/16	0.4874	0.4873	0.0483 e − 03
12/16	0.4578	0.4578	0.0562 e − 03
13/16	0.4301	0.4300	0.0628 e − 03
14/16	0.4040	0.4040	0.0683 e − 03
15/16	0.3796	0.3795	0.0726 e − 03

Table 2. Analysis of maximum absolute error.

N	Max. absolute error
16	1.480 e − 04
32	3.881 e − 05
64	9.936 e − 06

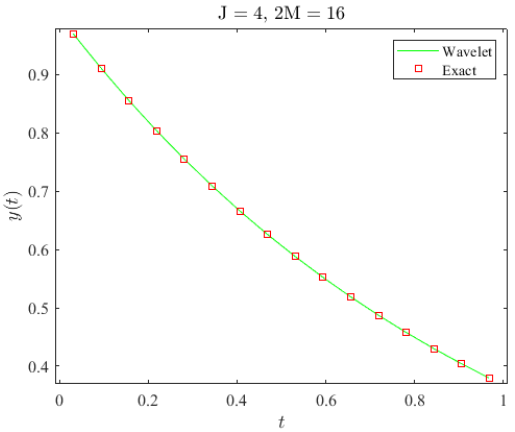


Figure 1. Haar wavelet solution for the problem 1, Case-A.

4.2 Problem 2 [Case-B]

Since Haar function is defined on [0,1], and better visualization of behavior of solution of fractional Mathieu differential equation demands a larger domain. Therefore, we need a transformation which allow (transform) the domain $[A, B]$ into $[0, 1]$. To do this we consider the solution of target differential equation be $y(x)$ on the domain $[A, B]$ with $y(A) = \alpha 1$ and $y'(A) = \beta 1$. Now, choose a new variable $x_1 = \frac{x-A}{B-A}$. Then the differential equation with respect to new variable is

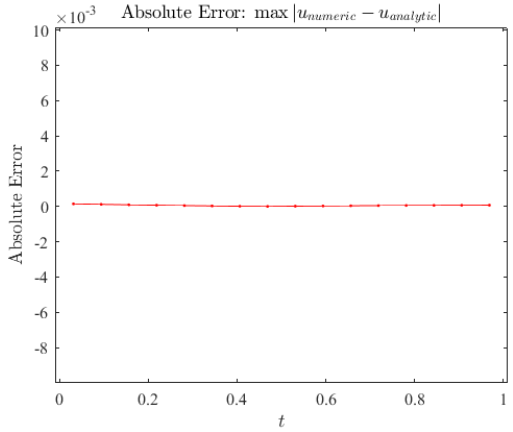


Figure 2. Error Analysis for the problem 1, Case-A.

given by

$$\frac{dy}{dx} = \frac{dy}{dx_1}\frac{dx_1}{dx} = \frac{1}{(B-A)}\frac{dy}{dx_1}, \tag{4.4}$$

and

$$\frac{d^2y}{dx^2} = \frac{1}{(B-A)^2}\frac{d^2y}{dx_1^2}, \tag{4.5}$$

The Mathieu fractional differential equation and initial conditions, now, will be transformed into a new equation with respect to new variable x_1 in the domain $[0, 1]$. Now, let the equation (1.2) defined over the domain $[0, 80]$. Then the equation (1.2) transformed into a new equation as:

$$\frac{1}{(80)^2}D^{\beta}y(x_1) + k\frac{1}{(80)}D^{\alpha}y(x_1) + (a - 2qcos(x_1))y(x_1) = f(x_1) \quad y(0) = \alpha 1, \quad y'(0) = \beta 1. \tag{4.6}$$

This case sets $k = 0$, $f(x) = 0$, $\quad a = 1, q = 0.1$, $\quad \alpha 1 = 0, \beta 1 = 0.5, \alpha = 1$ and $\beta = 2$ in equation (4.6). Figure 3 subsequently illustrates the approximate values across various values of $\alpha = 1$, $\quad \beta = 2$.

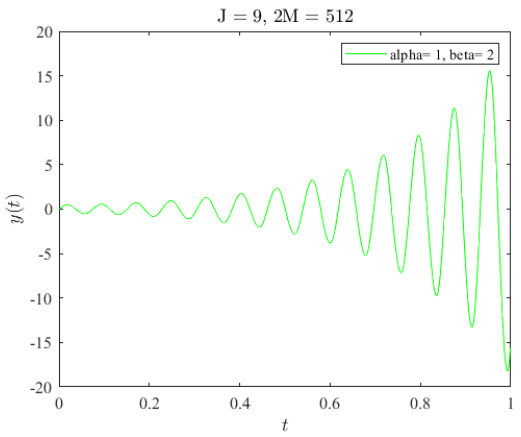


Figure 3. Haar wavelet solution for the problem 2, **Case-B** for α=1, β =2.

If we fix $\alpha = 1$ and change the values of β from 2 to 1.97 and 1.95, keeping other constants as it is, as mention above, we get the comparative changes shown in figure 4. From figure 3 and

figure 4, we can easily say that the solution of the Mathieu fractional equation is divergent, and it is very much compatible with the results given in [12]. Also, it can be analyzed that when the order of equation is two, it diverges faster while for non integer order, the rate of divergence is much lower. These two figures confirms that when order of equation is two, it is highly non linear and does not have stable solution [5] . Furthermore, when there is no damping force applied on the system, the solution of equation is divergent.

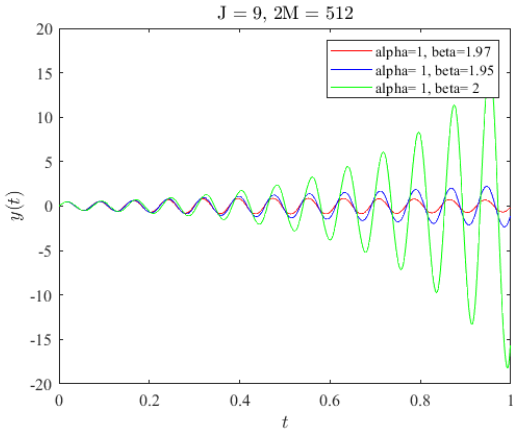


Figure 4. Haar wavelet solution for the problem 2, **Case-B** for $\alpha = 1,\ \beta = 2, 1.97, 1.95$.

4.3 Problem 3 [Case-A]

Consider the equation (4.6) with $k = 0.15$, $f(x) = 0$, $q = 0.1$, and $a = 1$, along with the initial values $y(0) = \alpha 1 = 0$ and $y'(0) = \beta 1 = 0.5$.

Figure 5 compares the approximate values of $y(x)$ for $\alpha = 1$ and $\beta = 2$. Here, we observe that the solution is consistent with [12] and converges to equilibrium very sharply when there is no characteristic parameter. The rate of convergence of solution is faster in this case comparing to the case when $q = 0.1$. If we take $\alpha = 1$ to 0.8 and 0.7, and β from 2 to 1.97 and 1.95 keeping

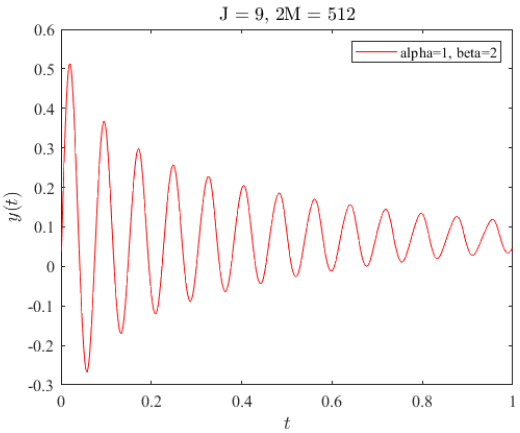


Figure 5. Haar wavelet solution for the problem 3, **Case-A** for $\alpha = 1,\ \beta = 2$.

other constants as it is as mentioned above, we see the comparative changes shown in figure 6. So, it is observed that the rate of convergence of the solution of equation is slower for integer values of α and β, and it converges sharply for non integer values of α and β.

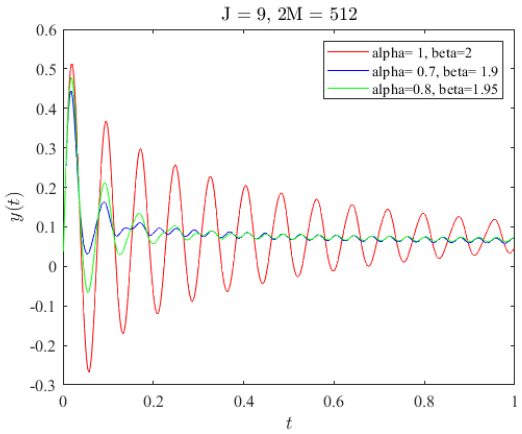


Figure 6. Haar wavelet solution for the problem 3, **Case-A** for $\alpha = 1, 0.8, 0.7, \beta = 2, 1.95, 1.9$.

4.4 Problem 4 [Case-C]

Consider equation (4.6) with the parameters set as follows: $k = 0.15$, $f(x) = 0$, $q = 0.0$, and $a = 1$. Additionally, we have the initial values $y(0) = \alpha_1 = 0$ and $y'(0) = \beta_1 = 0.5$. Figure 7 compares the approximate values of $y(x)$ for $\alpha = 1$ and $\beta = 2$.

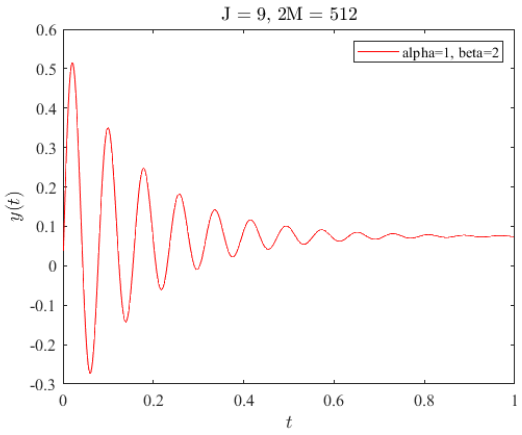


Figure 7. Haar wavelet solution for the problem 4, **Case-C** for $\alpha = 1, \beta = 2$.

If we take $\alpha = 1$ to 0.8 and 0.7, and β from 2 to 1.95 and 1.9, keeping other constants as it is, as mentioned above, we see the comparative changes shown in figure 8.

The approximate values of $y(x)$ for different values of α and β are shown in figure 6. Specifically, the values of $\alpha = 1, 0.7, 0.8$ and $\beta = 2, 1.9, 1.75$, respectively. In this scenario, the solution is consistent with the findings in [12] and exhibits convergence for $\alpha = 1$ and $\beta = 2$. Additionally, if we keep β fixed as two and vary α, as shown in figure 7, we observe that the solution converges with faster rate as compare to the previous case i.e., $\alpha = 1$, $\beta = 2$.

5 Conclusions

Present paper exhibits a novel fractional operational matrix of Haar wavelet and truncated Haar wavelet expansion to solve general form of nonlinear fractional Mathieu differential equations. The convergence of proposed scheme shows stability of the scheme. Test problems with different cases are discussed to simulate the solution of general form of target equation. The method demonstrates robustness and accuracy in approximating solutions to such equations. To enhance the precision of the results further, it is recommended to increase the number of collocation

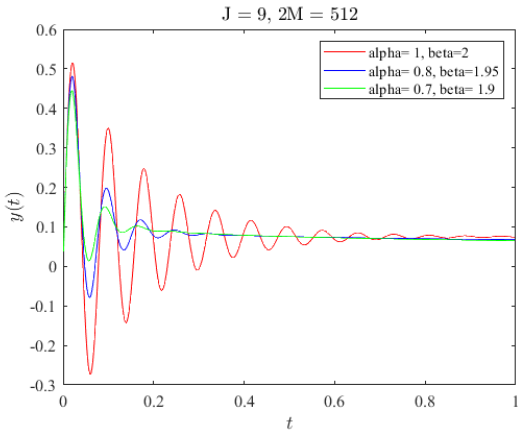


Figure 8. Haar wavelet solution for the problem 4, **Case-C** for $\alpha = 1, 0.8, 0.7, \beta = 2, 1.95, 1.9$.

points utilized in the numerical computations. This adjustment can lead to finer resolution and improved accuracy in the approximation of solutions to the fractional Mathieu differential equations. Diverse conditions show that the Haar wavelet offers a reliable and efficient means of tackling nonlinear equations, with the potential for even greater accuracy through the optimize selection of the collocation points.

References

[1] S. Chandrasekaran, P.A. Kiran. *Ocean Syst. Eng.*, **8(3)**,(2018), 345-360.

[2] J.J. Stoker. *Nonlinear Vibrations in Mechanical and Electrical Systems*, Interscience Publishers, New York, 1950.

[3] S.W. Liao, R.W. Yeung. *Proceedings of the 16th International Workshop on Water Waves and Floating Bodies*, Hiroshima, Japan, 2001.

[4] E. Mathieu. Memoire sur le movement vibratoire dune membrance de forme elliptique, *Journal de Mathematiques Pures Appliqués*, **13**, (1868), 137-203.

[5] R.H. Rand, S.M. Sah, M.K. Suchorsky. Fractional mathieu equation, *Commun. Nonlinear Sci. Numer. Simul.*, **15(11)**, (2010), 3254-3262.

[6] D. Younesian, E. Esmailzadeh, R. Sedaghati. Asymptotic solutions and stability analysis for generalized non-homogeneous Mathieu equation, *Commun. Nonlinear Sci. Numer. Simul.*, **12(1)**,(2007), 58-71.

[7] R.V. Bobryk, A. Chrzeszczyk. Stability regions for Mathieu equation with imperfect periodicity, *Physics Letters A*, **373(39)**, (2009), 3532-3535.

[8] J. Kalas, K. Kaderabek. Periodic solutions of a generalized Van der Pol-Mathieu differential equation, *Applied Mathematics and Computation*, **234**, (2014), 192-202.

[9] I. Kovacic, R. Rand, S.M. Sah. Mathieu′s equation and its generalizations: Overview of stability charts and their features, *Applied Mechanics Reviews*, **70(2)**, (2018), 020802.

[10] S.A. Wilkinson, N. Vogt, D.S. Golubev, J.H. Cole. Approximate solutions to Mathieu′s equation, *Physica E: Low-dimensional Systems and Nanostructures*, **100**, (2018), 24-30.

[11] H. Ghorbani, Y. Mahmoudi, F. Dastmalchi Saei. Numerical Study of Fractional Mathieu Differential Equation Using Radial Basis Functions, *Mathematical Modelling of Engineering Problems*, **7(4)**, (2020), 568-576

[12] P. Pirmohabbati, A.H. Refahi Sheikhani, H. Saberi Najafia, A. Abdolahzadeh Ziabari. Numerical solution of fractional Mathieu equations by using block-pulse wavelets, *Journal of Ocean Engineering and Science*, **4**, (2019), 299-307.

[13] M. Ruihong, w. Shaofang, S. Yongjun, S. Chundi. Stability Analysis of Fractional–Order Mathieu Equation with Forced Excitation, *Fractal Fract.*, **6(11)**, (2022), 633.

[14] I. Podlubny. *Fractional Differential Equations*, first edition, Academic Press, San Diego, (1990).

[15] H. Najafi, S. Mirshafaei, E. Toroqi. An approximate solution of the Mathieu fractional equation by using the generalized differential transform method (GDTM), *Applications and Applied Mathematics*, **7(1)**, (2012), 374-384.

[16] E. Abdelhalim, Elsayed, D.M., Aljoufi, M.D. Fractional calculus model for damped Mathieu equation: Approximate analytical solution, *Applied Mathematical Science*, **6(82)**, (2012), 4075-4080.

[17] S. Wen, Y. Shen, X. Li, S. Yang. Dynamical analysis of Mathieu equation with two kinds of van der Pol fractional-order terms, *Int. J. Non Linear Mech.*, **84**, (2016), 130-138.

[18] A.H. Nayfeh, D.T. Mook *Nonlinear Oscillations*,first edition, John Wiley and Sons, 1995.

[19] C. F. Chen, C. H. Hsiao. Haar Wavelet Method for solving Lumped and distributed parameter systems, *IEEE Proceeding Control Theory Appl.*,**144(1)**,(1997), 87-94.

[20] S. Imam., A. Imran, and S. Bozidar. The numerical solution of second order boundary value problems by collocation method with the Haar Wavelets, *Math. Comp. Model.*, **52**, (2010), 1577-1590.

[21] Hernandez E., G. Weiss. A first course on Wavelets. CRC Press, 1996.

[22] K. Ahmad, Abdullah. Wavelet Packets and Their Statistical Applications. Forum for Interdisciplinary Mathematics, 2018.

Author information

A. M. Jarrah, President, Philadelphia University
Department of Mathematics, Yarmouk University, Irbid, Jordan.
E-mail: ajarrah@yu.edu.jo

Jay Kishore Sahani, Department of Mathematics, D.A.V. Post Graduate College, Jai Prakash University, Chapra, Bihar, India.
E-mail: jay15delhi@gmail.com

Pankaj Sharma, Department of Mathematics, Pondicherry University, Pondicherry, India.
E-mail: pankajsharma@pondiuni.ac.in

Received: 2025-09-11
Accepted: 2026-04-06